Atmos. Chem. Phys., 17, 1775–1789, 2017
www.atmos-chem-phys.net/17/1775/2017/
doi:10.5194/acp-17-1775-2017

Atmospheric Chemistry and Physics
Open Access

Cleaning up the air: effectiveness of air quality policy for SO_2 and NO_x emissions in China

Ronald J. van der A[1,2], Bas Mijling[1], Jieying Ding[1,3], Maria Elissavet Koukouli[4], Fei Liu[1], Qing Li[5], Huiqin Mao[5], and Nicolas Theys[6]

[1]Royal Netherlands Meteorological Institute (KNMI), De Bilt, the Netherlands
[2]Nanjing University of Information Science and Technology, Nanjing, P.R. China
[3]Delft University of Technology, Delft, the Netherlands
[4]Laboratory of Atmospheric Physics, Aristotle University of Thessaloniki, Thessaloniki, Greece
[5]Satellite Environment Center, Ministry of Environmental Protection, Beijing, P.R. China
[6]Belgian Institute for Space Aeronomy (BIRA-IASB), Brussels, Belgium

Correspondence to: Ronald J. van der A (avander@knmi.nl)

Received: 24 May 2016 – Published in Atmos. Chem. Phys. Discuss.: 31 May 2016
Revised: 6 January 2017 – Accepted: 9 January 2017 – Published: 6 February 2017

Abstract. Air quality observations by satellite instruments are global and have a regular temporal resolution, which makes them very useful in studying long-term trends in atmospheric species. To monitor air quality trends in China for the period 2005–2015, we derive SO_2 columns and NO_x emissions on a provincial level with improved accuracy. To put these trends into perspective they are compared with public data on energy consumption and the environmental policies of China. We distinguish the effect of air quality regulations from economic growth by comparing them relatively to fossil fuel consumption. Pollutant levels, per unit of fossil fuel, are used to assess the effectiveness of air quality regulations. We note that the desulfurization regulations enforced in 2005–2006 only had a significant effect in the years 2008–2009, when a much stricter control of the actual use of the installations began. For national NO_x emissions a distinct decreasing trend is only visible from 2012 onwards, but the emission peak year differs from province to province. Unlike SO_2, emissions of NO_x are highly related to traffic. Furthermore, regulations for NO_x emissions are partly decided on a provincial level. The last 3 years show a reduction both in SO_2 and NO_x emissions per fossil fuel unit, since the authorities have implemented several new environmental regulations. Despite an increasing fossil fuel consumption and a growing transport sector, the effects of air quality policy in China are clearly visible. Without the air quality regulations the concentration of SO_2 would be about 2.5 times higher and the NO_2 concentrations would be at least 25 % higher than they are today in China.

1 Introduction

Satellite instruments can monitor air quality from space by mapping, for example, aerosols and tropospheric ozone, but they are especially useful for emission estimates in observing the relatively short-living gases nitrogen dioxide (NO_2) and sulfur dioxide (SO_2). For these two trace gases improved data sets have recently become available, enabling analysis of air quality time series on a national or provincial level with improved accuracy. Theys et al. (2015) presented a new data set of SO_2 column densities derived from the Ozone Monitoring Instrument (OMI) satellite instrument (Levelt et al., 2006). They conclude that the SO_2 concentrations derived from OMI agree on average within 12 % with ground observations. This data set strongly improves on earlier SO_2 data sets from satellites, which motivated this study. For NO_2, instead of using concentration data, we directly assess the emission data of nitrogen oxides ($NO_x = NO_2 + NO$) that were derived from satellite observations by Mijling and Van der A (2012) and remove the meteorological influences. The precision of the derived NO_x emissions per grid cell of $0.25° \times 0.25°$ is estimated as 20 % (Ding et al., 2016a).

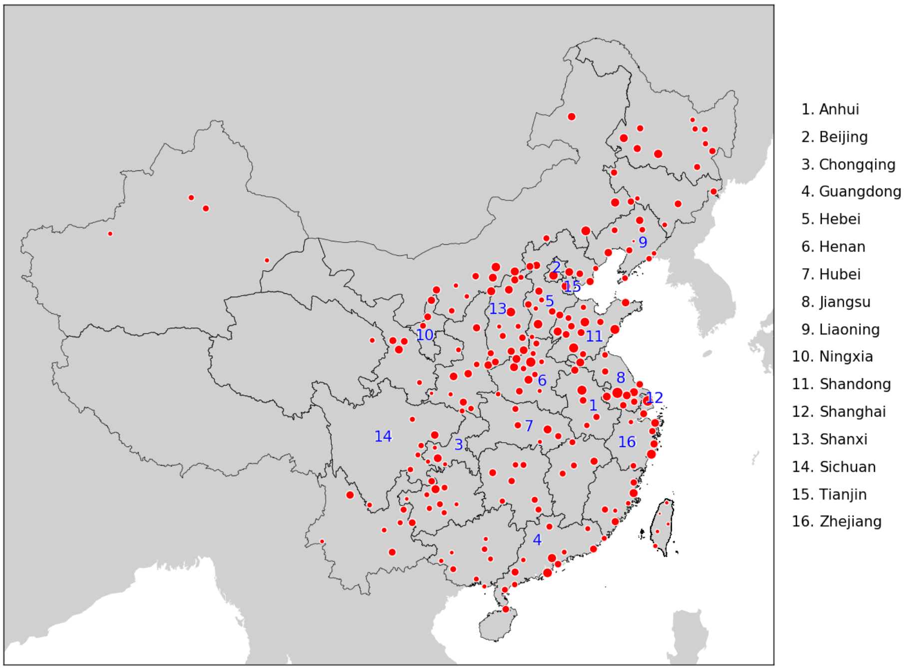

Figure 1. Location of power plants in China according to REAS v.2 (Kurokawa et al., 2013). The size of each dot indicates the emission of the power plants (power plants in close proximity are combined in a single dot). In addition, a list is given of the provinces mentioned in this study.

China is one of the largest emitters of SO_2 and NO_2 into the atmosphere because its large economy depends heavily on fossil fuels as an energy source. China alone is responsible for about 30 % of the total global emissions of SO_2 into the atmosphere (Klimont et al., 2013), while over 90 % of the SO_2 emissions are caused by coal consumption in China (Chen and Xu, 2010). Coal is mainly used by thermal power plants and in energy-intensive industry (e.g. steel, cement, and glass), and to a lesser extent residentially. SO_2 is also released by the use of oil and natural gas, but the sulfur content in these fuel types is much lower. Of these sources, power plants are responsible for about 30–40 % of all emissions and industry for another 50–60 % (He et al., 2012; ChinaFAQs project, 2012). According to the Multi-resolution Emission Inventory for China (MEIC) (http://www.meicmodel.org/) the source of SO_2 emissions in 2010 was 29.4 % from power plants, 57.7 % from industry, 11.7 % from residential, and 1.2 % from transport. Figure 1 shows the location of the 600 largest thermal power plants on the map of China, including a list of provinces mentioned in this study. At a global scale, volcanic activity is another important source of atmospheric SO_2. However, plumes of active volcanoes are seldom observed over China.

NO_x is released by more or less the same anthropogenic sources, i.e. the burning of coal or oil. The main difference to SO_2 is that traffic is a much more important source for NO_x. NO_x emission factors (i.e. emissions per fossil fuel unit) in the transport sector are generally much higher than emission factors in energy and industry, which makes traffic one of the major sources of NO_x in China. According to the MEIC inventory, 25 % of NO_2 in 2010 was released by traffic, 32 % by power plants, 4 % by residential sources and 39 % by industry, with the cement industry being the largest emitter in this sector.

To reduce SO_2 in China, the authorities have implemented several environmental regulations. The most important regulation was the desulfurization of coal-fired power plants in 2005/2006 (Xu, 2011). This was later followed in the 12th five-year plan (2011–2015) by stricter control on the implementation of the regulations; additional filtering efforts; switching to low-sulfur coal and petrol; phasing out obsolete capacity in coal-using industry; phasing out small-scale coal mining; and gradually using more oil, gas, and renewable energies instead of coal from 2011 onward. An overview of all regulations related to SO_2 is shown in Table 1, which includes the year in which the implementation began.

The regulation of NO_x was started much later than for SO_2. The 12th five-year plan mentioned the intention to reduce NO_2 by 10 % (target) (ChinaFAQs project, 2012); from 2011 onward NO_x filtering systems were installed, mainly at power plants but also for heavy industry. These regulations for NO_x were announced in 2013 in the Air Pollution Prevention and Control Action Plan (CAAC, 2013). According to Liu et al. (2016b) selective catalytic reduction (SCR) equipment was installed in this period and grew from a penetration of about 18 % in 2011 to 86 % in 2015. SCR equip-

Table 1. Environmental regulations of the Chinese national government to reduce SO_2 in the air.

Start year of implementation	Regulation	Reference
2005–2006	Desulfurization techniques in power plants	Li et al. (2010)
2005–2012	Closure of several of the most polluting power plants	Liu et al. (2015)
2008	Stricter control of implementation of desulfurization in power plants	Xu et al. (2011) Liu et al. (2015)
2011	Use of more gas and renewable energies instead of coal	NBSC (2015)
January 2012	New emission standard of air pollutants for thermal power plants	MEP (2015)
2013	Mandatory SO_2 filtering of small-scale coal-fired industry	Zhang (2013), NDRC (2013)
End of 2013	Stricter control of environmental policy	CAAC (2013), State Council (2014)
End of 2013	Further desulfurization in industry	CAAC (2013), NDRC (2013)
2014	Phasing out small-scale coal-fired boilers	CAAC (2013), State Council (2014)
2014	Closure of 2000 small-scale coal mines	Zhu (2013)
End of 2014	Use of low-sulfur coal	State Council (2014)
End of 2014	Cap on coal consumption	State Council (2014)

Table 2. Environmental regulations of the Chinese national government to reduce NO_x emissions.

Year of implementation	Regulation	Reference
2011–2015	Installation of selective catalytic reduction (SCR) equipment at power plants; in 2013 the SCR equipment was installed in about 50 % of all power plants	Liu et al. (2016b), CAAC (2013)
2007	China 3 (Euro 3) emissions standards for cars, nationwide	Wu et al. (2017)
2011	China 4 (Euro 4) emissions standards for gasoline cars, nationwide	Wu et al. (2017)
2015	China 4 (Euro 4) emissions standards for diesel cars, nationwide	Wu et al. (2017)

ment in power plants are expected to reduce the emissions of the power plant by at least 70 % (ICAC, 2009). The SCR installation is the most significant measure taken to reduce the NO_x emissions, and it largely coincides with the peak year of observed NO_2 concentrations (Liu et al., 2016b). At the same time, China has implemented several new national emission standards for cars during the time period of our study (see Table 2). The change from China 3 to China 4 standard for cars in the period 2011–2015 reduces the maximum allowed amount of NO_x emissions for on-road vehicles by 50 % (Wu et al., 2017). More strict regulations for on-road vehicles (e.g. a ban on older polluting cars) were introduced on a city level, e.g. in Beijing, rather than nationwide. To our knowledge no regulations for ship emissions have been announced. Strong regulations have also been enforced during specific events like the Olympic Games in 2008, the Shanghai World Expo in 2010, the Nanjing Youth Olympic Games in 2014, and the APEC meeting in 2014, but those regulations were mostly of a temporary nature as shown by, for example, Mijling et al. (2013) for the Olympic Games in 2008.

To study the efficiency of the environmental policies, we analysed satellite observations of SO_2 and tropospheric NO_2 of the last 11 years. SO_2 satellite observations over China have been studied earlier by Lee et al. (2011), Li et al. (2011), He (2012), Yang et al. (2013), Fioletov et al. (2015), and Krotkov et al. (2016). Satellite observations are very useful for SO_2 trend studies, as recently McLinden et al. (2016) showed that bottom-up inventories are underestimating SO_2 emissions worldwide by about 0–10 %. NO_2 satellite observations over China have been evaluated by, for example, Richter et al. (2005), van der A et al. (2006), Zhang et al. (2012), and Krotkov et al. (2016). All these studies showed a strong increase in NO_2 over East China. On a city scale or regional level, trends are analysed and reported by Gu et al. (2013), Schneider et al. (2015), and Duncan et al. (2016). Although some cities have already showed a decreasing trend, notably in the Pearl River Delta, an overall decrease in NO_2 concentrations in China has only recently been observed by Irie et al. (2016), Liu et al. (2016b), and de Foy et al. (2016). To exclude meteorology as a factor for variability in NO_2, several authors have evaluated NO_x emissions instead. Emission estimates of NO_x over China have been analysed by Stavrakou et al. (2008), Kurokawa et al. (2009), and more recently by Mijling et al. (2013) and by Liu et al. (2016a).

In these studies, whether of concentrations or emissions, linear trends of the air pollutants are often used. Here, however, we will relate changes derived on a provincial level for China to the energy consumption and the environmental policies of the country. This gives insight into the efficiency of the applied air quality policies and regulations. We apply this to NO_x emissions instead of concentrations for the period 2007 until 2015. The comparison of SO_2 trends with those of NO_x emissions enables us to distinguish environmental policies specifically applied on coal-based industry and power plants with general environmental measures and trends in traffic.

2 Observational data

2.1 Satellite observations of SO_2

SO_2 is observed in the UV spectral range of satellite observations of SCIAMACHY (on Envisat), GOME-2 (on METOP-A) and OMI (on EOS-AURA). SO_2 retrieval algorithms have been developed earlier for GOME-1 by Eisinger and Burrows (1998), for SCIAMACHY by Lee et al. (2008), and for GOME-2 and OMI by Krotkov et al. (2006). Recently a new retrieval algorithm has been developed (Theys et al., 2015) that improves the precision of the SO_2 data for OMI by a factor of 2, allowing us to derive more accurate trends based on OMI. The retrieval method is based on a differential optical absorption spectroscopy (DOAS) scheme to determine the slant columns from measured spectra in the 312–326 nm spectral range, which are then background-corrected and converted to vertical columns using an air mass factor (AMF). The AMF is calculated with the radiative transfer model LIDORT (LInearized Discrete Ordinate Radiative Transfer model). More details about the retrieval procedure are described in Theys et al. (2015). The operational algorithm of NASA for SO_2 from OMI has also recently been improved. This algorithm and the algorithm of Theys et al. (2015) have a very comparable performance as shown by Fioletov et al. (2016). For this study, the algorithm of Theys et al. (2015) has been applied to the observations of the OMI instrument (Levelt et al., 2006) for its whole mission from 2004 onwards.

To improve the quality of the OMI SO_2 data we exclude observations with a cloud fraction of more than 50 % or with a fitting chi-square higher than 1. The solar zenith angle is limited to 75° and the viewing angle to 50°. Since the OMI instrument has been suffering from the so-called row anomaly since 2007 (KNMI, 2012), we filter the affected rows (24–49, 54–55) in the same way for all years in the time series.

As we focus on anthropogenic SO_2, the SO_2 data for 15 June–9 July 2011 have been removed because of contamination with volcanic SO_2 from the eruption of the Nabro volcano in Africa and the transport of its plume to China (Brenot et al., 2014).

As a first step in our study we have made monthly means for the whole data set by averaging and gridding the data to a resolution of $1/8°$ by $1/8°$. The gridding algorithm takes into account the area of each satellite footprint overlapping the grid cell. The resulting data set is a time series of monthly means for the time period October 2004 to December 2015.

For comparison we also use the official ESA SCIAMACHY/Envisat SO_2 version product SGP 5.02; and the standard data from the GOME-2/Metop-A version GDP 4.7, as developed within the EUMETSAT Satellite Application Facility for Atmospheric Composition and UV radiation (O3MSAF) project and distributed by http://atmos.caf.dlr.de/gome2/. The data of these instruments are noisier than the OMI data sets because of the lower spatial coverage, different fit window, and the lower signal-to-noise ratio of the SCIAMACHY and GOME-2 instruments. Therefore, their quality-controlled monthly mean SO_2 data have been recalculated by spatially averaging, for each grid cell, the data from the eight surrounding neighbouring cells, hence creating a smoothed SO_2 field. For details on the methodology and findings, refer to Koukouli et al. (2016).

2.2 NO_x emission estimates from satellite observations

For NO_x emission data we use the results of an update (version 4) of the DECSO (Daily Emission estimates Constrained by Satellite Observation) algorithm developed by Mijling and van der A (2012). DECSO calculates emissions by applying a Kalman filter for the inversion of satellite data and a regional chemical transport model (CTM) for the forward model calculation. It takes transport from the source into account with a semi-Lagrangian approach. The CTM we use is CHIMERE v2013 (Menut et al., 2013) with meteorological information from the European Centre for Medium-Range Weather Forecasts (ECMWF) with a horizontal resolution of approximately 25 km × 25 km. The DECSO algorithm is applied to OMI NO_2 observations derived by the DOMINO v.2 algorithm (Boersma et al., 2011). The latest improvements of the DECSO algorithm resulting in version 4 are described by Ding et al. (2015, 2016a). The monthly average emission data over China we use are available at 0.25° resolution for the period 2007–2015 on the web portal www.globemission.eu.

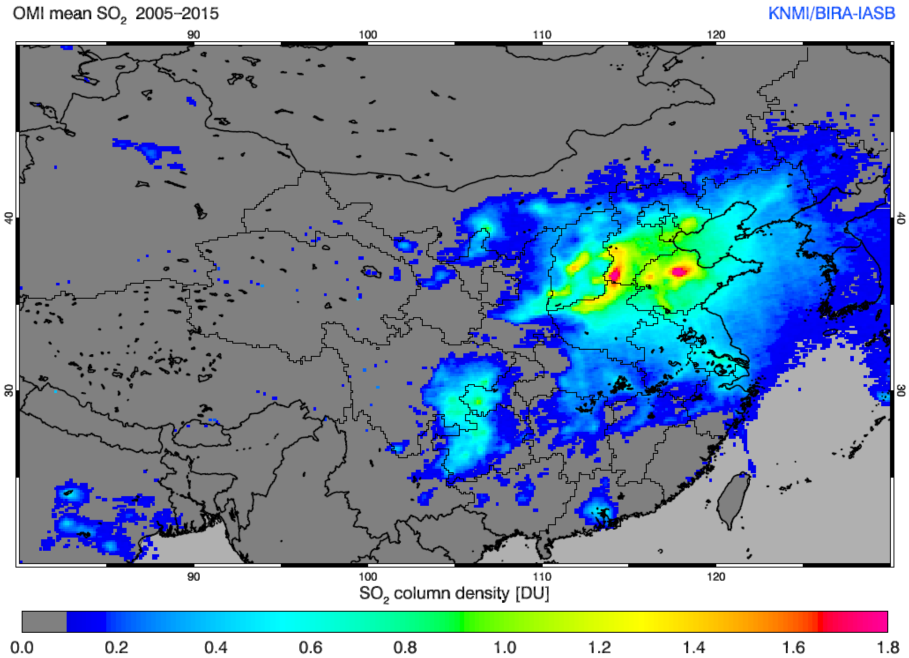

Figure 2. Average SO_2 concentrations for the period 2005 to 2015 as observed by the OMI satellite instrument. Data below 0.1 DU are masked (grey).

3 Temporal analysis over China

3.1 Sources of SO_2 and NO_x in China

The multi-annual mean of SO_2 for 2005–2015 is shown in Fig. 2. As the lifetime of SO_2 is relatively short (typically 4–48 h) (Lee et al., 2011; Fioletov et al., 2015); the observed SO_2 concentrations are a good proxy for the location of SO_2 emissions. Regions with large SO_2 concentrations are south Hebei, the province of Shandong (around the city of Zibo) and the region around Chongqing. South Hebei is a region with many power plants just east of the mountainous coal-mining area in Shanxi. The hotspot in the Shandong province is related to a strongly industrialized area with substantial coal-using industry. Both coal mines and heavy industry are located in the Chongqing region.

Rather than located at hotspots, high NO_2 concentrations are more distributed over the east of China, mainly because traffic is an important source of NO_x emissions (see Fig. 3a). The underlying NO_x emissions are shown in Fig. 3b. Like the SO_2 concentrations, NO_x emission spots can be found at the location of large power plants. Also clearly visible are the megacities of China, ship tracks along the coast, and sources along the large rivers.

3.2 SO_2 trends over China

To construct time series of SO_2 we have averaged the data to annual means of the vertical columns derived from OMI. From these annual mean SO_2 data we constructed time series for each province (see Table A1). Figure 4 shows the mean normalized time series for the 10 provinces with the highest total SO_2 column densities (i.e. Tianjin, Shandong, Hebei, Shanxi, Henan, Beijing, Jiangsu, Shanghai, Anhui, and Liaoning), together responsible for 60 % of all ambient SO_2 in China. The individual time series are drawn as thin grey lines. The minimum and maximum of these time series for each year are shown in the grey shaded area to indicate the variability. The time series of Shanghai is the lowest grey line of the 10 series; thus the reductions have been strongest in this province since 2005. Apart from Ningxia province, all provincial time series show very similar patterns. In general, the SO_2 concentrations were at a maximum in the year 2007, when the start of a decreasing trend is visible in China. Despite some fluctuations the SO_2 concentrations remain relatively constant from 2010 until 2013, whereafter they are decrease again.

A different trend is observed for Ningxia, a province in the mid-northern region of the country with a relative low population density and large coal resources. Here an increasing trend emerges for the years starting from 2010, when several new coal power plants were put into operation. A list of the largest power plants (with a capacity of more than 600 MW) and the start year of their operation is shown in Table 3. From 2012 onward, the more stringent SO_2 emission regulations also started to have an effect in Ningxia.

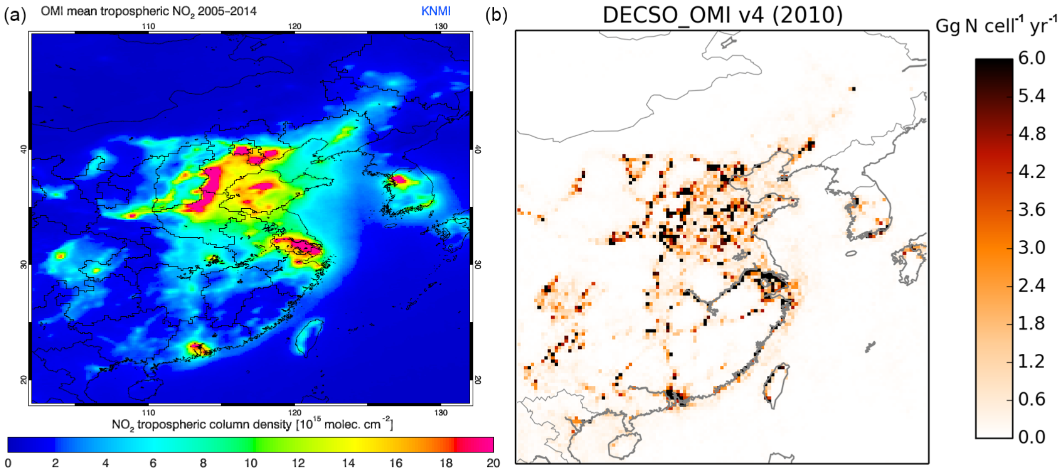

Figure 3. (a) The averaged tropospheric NO_2 concentrations over China measured by OMI in the period 2005–2014. **(b)** The NO_x emissions in the year 2010 derived from OMI satellite observations.

Table 3. Main power plants in Ningxia province (> 600 MW). Data collected from www.sourcewatch.org.

Power plant	Capacity (MW)	In operation since	Remark
CPI Linhezhen	700	unknown	
Daba-1	1200	< 2000	
Daba-2	1100	unknown	An extension of Daba-1
Ningxia Zhongning-2	660	2005–2006	
Guodian Shizuishan-2	1980	2006	
Ningdong Maliantai	660	2006	
Huadian Ningxia Lingwu units 1 and 2	1200	2007	
Guodian Dawukou	1100	2010	Extension of the original 440 MW plant
Guohua Ningdong	660	2010	
Ningxia Liupanshan	660	2010	
Huadian Ningxia Lingwu units 3 and 4	2120	2010–2011	
Shenhua Yuanyang Lake	1320	2010–2011	
Shuidonggou	1200	2011	
Ningdong Younglight	660	2013	

3.3 NO_x emission trends over China

National NO_x emission trends show a different pattern than those of SO_2. We observe an increasing trend until about 2012, with the exception of the year 2009, which is related to regulations started at the Olympic Games in 2008 (Mijling et al., 2009) and the global economic crisis, which briefly slowed down Chinese economic growth. Total NO_x emissions in East China reached their peak levels in 2012, and have stopped increasing since this year. While the economy kept growing after 2012, the emission of NO_x slowly decreased again as a result of the air quality regulations described in Sect. 1. According to the DECSO emission inversion, in 2015 the NO_x emissions were 4.9 Tg N yr^{-1}, which is 22.8 % lower than in the peak year, 2012. However, the 2015 emissions were still 14.1 % higher than in the reference year, 2007. The trends per province (see Table A2) show very similar patterns, with only the starting year (the year with maximum NO_x emissions) of the decrease in emissions varying over the provinces. Events like the Olympic Games in Beijing in 2008 and the World Expo in Shanghai in 2010, when temporary strict air quality regulations were enforced, can be recognized in this table as years with significantly lower emissions for these provinces. In Fig. 5a, the normalized (to the year 2007) time series of annual NO_x emissions for East China (102–132° E, 18–50° N) is shown in similar way to SO_2 in Fig. 4. The mean, minimum and maximum of the 10 provinces with the highest NO_x emission are shown (Shandong, Hebei, Henan, Jiangsu, Guangdong, Shanxi, Zhejiang, Anhui, Sichuan, and Hubei), together responsible for 65 % of all Chinese NO_x emissions. The thin grey lines show the times series for the individual 10 provinces, where the lower line represents Guangdong. Figure 5b shows the peak year for each province. Provinces

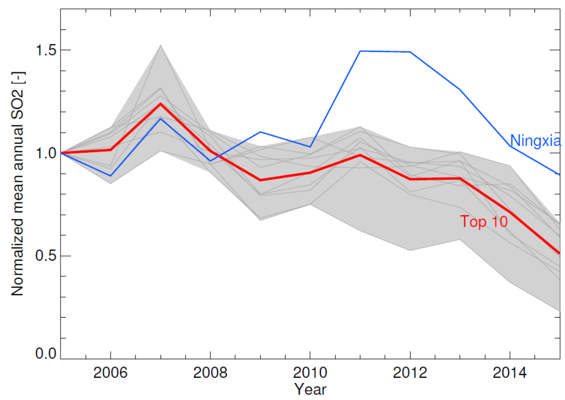

Figure 4. Time series (red line) of the annual mean of the 10 provinces with the highest SO_2 concentrations derived from the OMI satellite observations. The time series are normalized to their value in 2005. The grey area indicates the maximum range of the individual values of the times series of each of the 10 provinces. The thin grey lines show the individual time series of those provinces. The province of Ningxia has a distinct deviating trend, here shown in blue.

where air pollution regulations, e.g. for traffic, received a lot of attention at an early stage, like Beijing and Shanghai, reached their maximum before 2011. Most industrialized regions show their peak in the years 2011–2013. Some of the less developed and populated provinces show a maximum in 2014, which means that their decrease in NO_x emissions is very recent. Regional variations are mainly due to the fact that regulations for the NO_x emission reductions, for instance in traffic or power plants, are determined and implemented on a provincial level (Liu et al., 2016b). For the province of Ningxia we see a pattern occuring that is very similar to that of SO_2, which shows for this low-population-density province that traffic plays a small role and the trend is determined by the operation of newly built power plants.

3.4 Air pollution in relation to fossil fuel consumption

To relate the observed SO_2 and NO_x reduction to environmental regulations we have to take into account the coal and oil consumption in the same time period. The total coal consumption in standard coal equivalent (SCE) units per year for China and the total oil consumption (also in SCE units) are shown in Fig. 6, based on data of NBSC (2015). According to Guan et al. (2012) and Hong et al. (2016) the sum of coal consumption of all provinces is more accurate than the number provided for the whole of China; thus we use the provincial totals for coal consumption. For NO_x emissions the transport sector plays an important role; ships especially are one of the largest NO_x emitters per fuel unit in the transport sector. The total freight transport almost doubles every 6 years in China.

Since the burning of coal and oil constitutes the dominant sources of SO_2 and NO_x emissions, we can consider the total emissions of these air pollutants as the product of the national use of coal and oil (activity) and the average emission factor of one unit of coal/oil. The effectiveness of environmental regulation will be reflected in a decrease in this emission factor. Therefore, we divide the annual SO_2 column measured from satellites and the annual NO_x emissions by the annual coal and oil consumption in China. In this way we get a measure of the emitted SO_2 or NO_x per unit (SCE) of fossil fuel consumption reflecting the Chinese environmental policy. The results are shown in Fig. 7. One might argue that SO_2 is more related to coal than oil, but division by only coal yields the same results. In our analysis we omit gas consumption since this is very limited in China and hence does not affect the results significantly.

We focus here mainly on the results for OMI, because of the instrument's high spatial resolution and lack of instrumental degradation. However, SO_2 data of the SCIAMACHY and GOME-2 instrument are also added in Fig. 7 to be able to further look into the past (starting in 2003) and to verify the results of OMI. The SO_2 data of SCIAMACHY and GOME-2 are averaged over the summer months (April–September). The remaining monthly means are excluded from the analysis due to a lower accuracy at higher latitudes, and a large part of the higher latitudes is missing due to snow cover. For OMI each data point is averaged over 12 months and the total area of China, which reduces the root-mean-square error to a negligible level. Biases among all instruments are removed by normalizing the values to those in reference year 2007. Up to 2009, the results agree fairly well. After 2009, we see the results of GOME-2 and OMI for SO_2 slowly diverge in time, which might be a result of the instrument degradation of the UV spectra of GOME-2 after 2009 (Munro et al., 2016).

Changing weather conditions from year to year can affect the results for SO_2 concentrations, and when the weather conditions are different during the overpass of SCIAMACHY and GOME-2 (around 09:30 LT, local time) than those at the overpass of OMI (around 13:30 LT), this can lead to differences between the instruments. The global coverage of SCIAMACHY is once every 6 days and for GOME-2 and OMI almost daily. The limited number of samples for SCIAMACHY makes these data more sensitive to weather conditions. Note that, due to the nature of the inversion algorithm, the NO_x emission data are in general not sensitive to meteorological variability.

For SO_2 we see a large decrease in the years 2008 and 2009, while the desulfurization programme of the 11th five-year plan had already started in 2005/2006, when the authorities began to reduce SO_2 emissions by installing desulfurization devices in many power plants (Lu et al., 2010). In 2006 SO_2 monitoring devices were also installed in the chimneys of the power plants. This resulted in a decrease in SO_2 emissions from 2006, while the much larger decrease in SO_2 in 2008–2009 reflects the stronger government control at that time on the actual use of the equipment (Xu et al., 2011). Af-

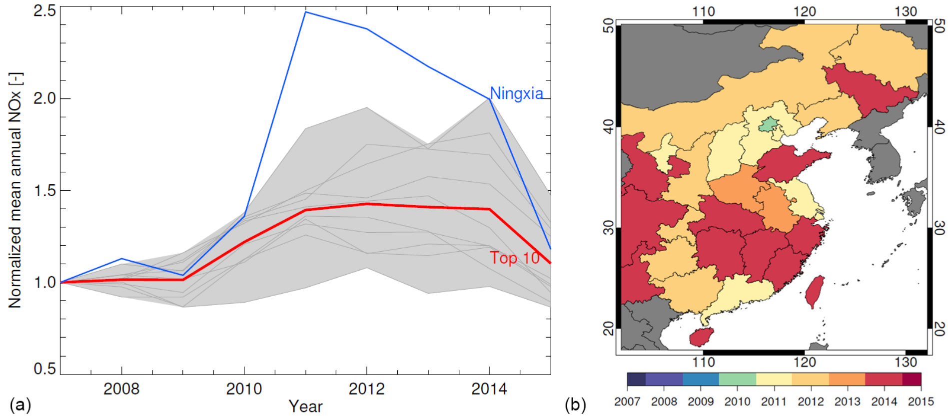

Figure 5. (a) The annual total NO_x emission estimates for the last 9 years for the top 10 highest NO_x-emitting provinces in East China. Emissions are derived with DECSO V4 using OMI observations. The thin grey lines show the individual time series of those provinces. **(b)** Peak year of the NO_x emissions per province.

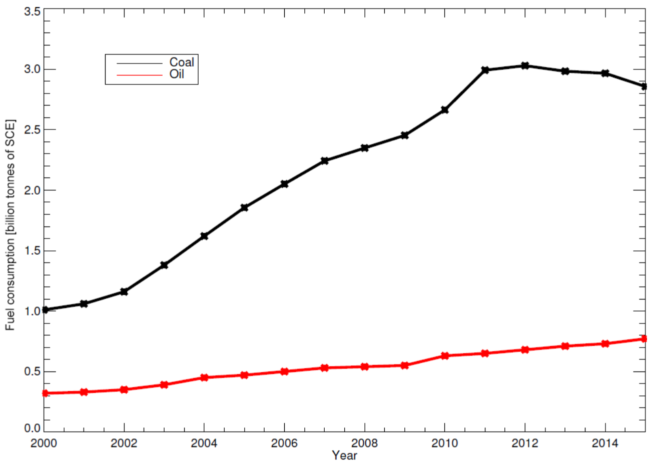

Figure 6. In black the annual coal consumption. In red the annual oil consumption for China.

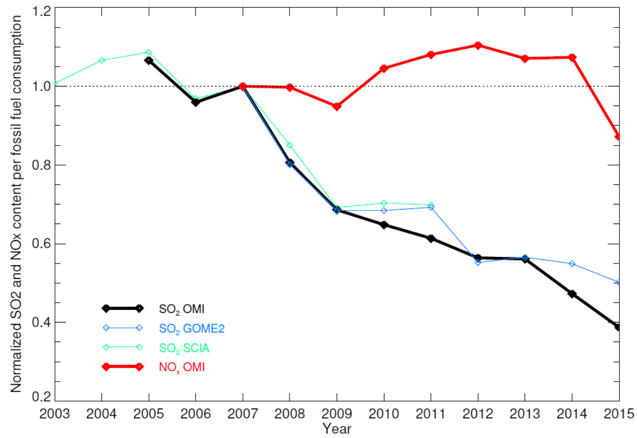

Figure 7. Time series of the ratio of the mean SO_2 columns and the fossil fuel consumption in China based on observations of OMI (black), SCIAMACHY (green), and GOME-2 (blue). The ratios of the annual NO_x emissions and the fossil fuel consumption are based on observations of OMI (red). All time series are normalized to the year 2007.

ter 2009, the SO_2 content per consumed coal unit only slowly decreases until 2011. From 2012 onwards we see a stronger annual decrease in SO_2. This coincides with the 12th five-year programme; when new measures were taken to upgrade the coal quality, to modernize the industry, and to put more effort on law enforcement. The enforcement of laws in the last few years concerning the prohibition of flue gas bypass and the use of desulfurization devices in the steel industry played an especially important role.

For the NO_x emissions the total annual emissions are used and divided in the same way as for SO_2 by the total coal and oil consumption. Here, however, we should keep in mind that the transport sector (especially by shipping) emits much more NO_x per fuel unit than the power and industrial sectors (see, e.g., Zhao et al., 2013). Thus, the percentage of the total fuel used by transport is relevant for the graph of NO_x. In the early years we see, in general, a small increase in NO_x emissions per fuel unit due to the increasing fraction of the transport sector in fuel usage. Exceptions are the year 2009 and the recent year 2015. The year 2009 coincides with the global economic crisis (Lin and McElroy, 2011), when there was less export of goods from China. This especially affected the transport sector, mostly transport over water, as shown in De Ruyter de Wildt et al. (2012). Faber et al. (2012) and Boersma et al. (2015) showed that the economic crisis also resulted in a significant reduction in the average vessel speed to save fuel used by ship transport. This not only caused a shift in source sectors but also in general led to lower NO_x per fuel values. This explains the dip in pollution per fuel unit in 2009. After 2009 the NO_x per fossil fuel is slowly increasing because the transport sector is growing faster than the energy sector and has a higher emission factor. Statistics of the NBSC (2015) show that transport is growing by a factor of 2 every 5–6 years (Wu et al., 2017). After 2012 the gradual increase in NO_x per fuel slowly stops, and the year 2015 shows a sharp decline in NO_x per fossil fuels unit. This can be directly related to the rapidly growing installation of SCR equipment at power plants since 2012 and to a lesser extent to the introduction of new emission standards for cars, as shown by Liu et al. (2016). This strong reduction in NO_x for 2015 and the equally strong reduction for SO_2 in 2014 and 2015 are a result of very effective recent environmental regulations in the last years in China. By comparing the efficiency level in 2015 with earlier levels, we can conclude from Fig. 7 that, without these air quality regulations, SO_2 concentrations would today be about 2.5 times higher. For NO_x per fossil fuel we were expecting a gradual growth after 2012 because of the continuing relative growth of the transport sector. Keeping this in mind we compare the years 2015 with 2012 and conclude that without air quality regulations the NO_2 concentrations would be at least 25 % higher in China today.

On a provincial scale we can, in principle, do similar analyses, but unfortunately the provincial energy consumption related to coal and oil has a very high uncertainty due to inconsistencies in interprovincial imports and exports (Hong et al., 2016). We see this reflected in a high variability in the annual provincial data and sometimes missing data. The data have high uncertainties especially for oil consumption (Guan et al., 2012; Hong et al., 2016). Therefore, we have only analysed the five provinces with dominating coal consumption as shown in Fig. 8. In this graph we excluded Guizhou province because of its difficult-to-interpret coal consumption in 2011 as a result of large power shortages (NBSC, 2015; Sun and Zhou, 2011). For SO_2 per fossil fuel unit we see that all provinces follow the national trend. For NO_x per fossil fuel we see more variation per province, depending on the role of transport. Most of these coal-consumption-dominated provinces start their decreasing trend from 2011, reflecting the national programme on SCR installations starting that same year. It is interesting to see that the commissioning of new power plants in 2011 causes a strong increase in both SO_2 and NO_x in Ningxia province (see Figs. 4 and 5a). However, when compensating for fossil fuel usage, one can see that the same national air quality regulations are applied here, as the trend in Fig. 8 shows the same pattern as for other provinces. This shows the strength of the presented method to assess the efficiency of air pollution regulations.

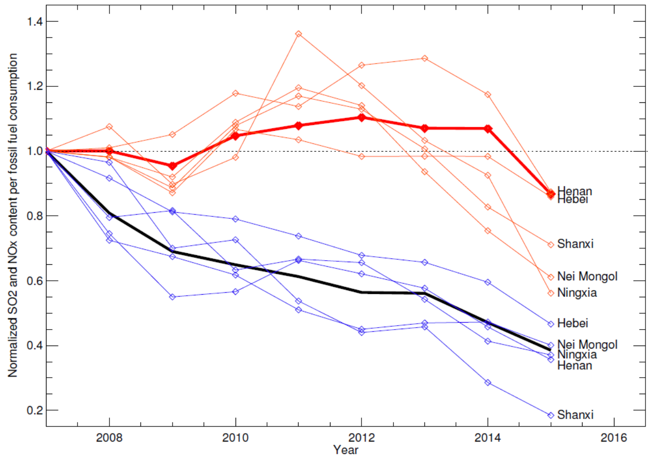

Figure 8. Same graph as Fig. 7 but with time series for the provinces Hebei, Henan, Nei Mongol, Ningxia, and Shanxi included. Time series per province of the ratio of the mean SO_2 columns and the fossil fuel consumption are drawn in blue. The ratios of the annual NO_x emissions and the fossil fuel consumption per province are shown in red. All time series are normalized to the year 2007 and based on OMI observations.

4 Discussion

The current developments in data products derived from satellite observations provide high-quality time series of the air pollutants NO_x and SO_2. Although the mean of observed SO_2 columns is not linearly related to the SO_2 emissions because of the influence of the weather, it can still be argued that these satellite data products, whether concentrations or emissions, provide a fair comparison over the various regions from year to year. By comparing these time series with fossil fuel energy consumption we find that the economic growth is removed from the equation and we can monitor the effectiveness of air quality policies. We foresee that this method will become a valuable tool for policy makers concerning air quality regulations.

For China we see patterns in the trends of SO_2 that are similar for all provinces. In 2006 a nationwide implementation of desulfurization installations started. However, the effects are only visible in 2008 and 2009, when a strict control by the Chinese authorities on the actual use of the desulfurization installations started. In 2009, we see the effect of the air quality regulations for SO_2 and NO_x resulting from the global economic recession at the end of 2008. The increasing relative contribution of the transport sector to the NO_x emission slowly increases the amount of NO_x per fossil fuel unit after 2009. After 2011 we see a steadily decreasing SO_2 pollution per fossil fuel unit caused by various Chinese environmental regulations. In the last year of our time series, 2015, a clear effect becomes visible of very recent regulations for NO_x emissions from power plants and heavy industry. The fit of linear trends often used in earlier studies is therefore no longer applicable to the Chinese situation.

For the first time it is shown from satellite observations that not only NO_2 concentrations in China but also NO_x emissions in all Chinese provinces have been decreasing in the last two years of our study. Showing this decreasing trend for emissions of NO_x rules out any meteorological influences that affect concentrations. By the novel method of dividing these NO_x emissions by the fossil fuel consumption and thereby showing the decreasing trend in emission factors in China, we also exclude the effect of economic changes, which has always been the driving factor in the trend of emissions in China in the past decades. We have given a complementary new overview of the main national air quality regulations in China from which changes in the emission factors of NO_x and SO_2 can be understood and clarified. These trends in emission factors of NO_x and SO_2 based on satellite observations might also be applied to verification of existing emission factors.

The availability of high-quality satellite data for the last 10 years is especially interesting for China, where the situation is rapidly changing. For instance, in Europe and Japan, desulfurization started much earlier, when these satellite data were not yet available. On the other hand, in India SO_2 and NO_x emissions are still growing and possible new regulations can be monitored in the years to come, with even better quality, using forthcoming sensors such as TROPOMI on board Sentinel-5 Precursor.

Despite the growing use of coal and oil in the last 10 years in China we have recently seen reduced emissions per fuel unit. This decreasing trend in both SO_2 and NO_x for China is likely to continue in the coming years for which the Chinese national government has announced less use of coal, more environmental regulations for SO_2 and NO_x, and stricter reinforcement of control of environmental policies.

5 Data availability

The SCIAMACHY and OMI SO_2 data used in this study can be obtained by contacting co-author Nicolas Theys (nicolas.theys@aeronomie.be). The GOME-2/Metop-A SO2 data (version GDP 4.7) are available at http://atmos.caf.dlr.de/gome2/ (Valks, 2016). The NO_x emission data is available at http://www.globemission.eu/region_asia/datapage.php (Ding et al., 2016b).

Appendix A

Table A1. Annual SO_2 column densities (DU/grid cell) per province observed by OMI.

Province	2005	2006	2007	2008	2009	2010	2011	2012	2013	2014	2015
Anhui	0.625	0.586	0.953	0.637	0.499	0.567	0.671	0.553	0.602	0.379	0.280
Beijing	0.753	0.829	0.989	0.711	0.778	0.749	0.850	0.673	0.634	0.640	0.491
Chongqing	0.514	0.509	0.530	0.567	0.580	0.580	0.492	0.370	0.469	0.269	0.136
Fujian	0.099	0.123	0.196	0.135	0.104	0.113	0.112	0.080	0.107	0.076	0.064
Gansu	0.144	0.136	0.150	0.130	0.135	0.123	0.134	0.127	0.131	0.105	0.103
Guangdong	0.251	0.257	0.280	0.239	0.171	0.177	0.138	0.095	0.118	0.086	0.080
Guangxi	0.199	0.203	0.270	0.236	0.127	0.190	0.179	0.092	0.134	0.091	0.072
Guizhou	0.424	0.478	0.532	0.516	0.418	0.424	0.357	0.261	0.345	0.167	0.100
Hainan	0.098	0.086	0.091	0.092	0.060	0.090	0.106	0.027	0.087	0.055	0.000
Hebei	0.903	0.931	0.996	0.908	0.874	0.881	0.922	0.863	0.844	0.716	0.540
Heilongjiang	0.134	0.141	0.144	0.142	0.124	0.138	0.154	0.162	0.125	0.134	0.135
Henan	1.036	0.920	1.222	0.938	0.709	0.778	0.992	0.827	0.762	0.585	0.439
Hubei	0.487	0.477	0.603	0.490	0.342	0.386	0.479	0.365	0.378	0.288	0.176
Hunan	0.364	0.330	0.448	0.371	0.270	0.281	0.320	0.240	0.259	0.180	0.112
Jiangsu	0.847	0.782	1.054	0.917	0.678	0.716	0.871	0.687	0.735	0.524	0.326
Jiangxi	0.272	0.278	0.373	0.267	0.202	0.222	0.244	0.197	0.230	0.184	0.136
Jilin	0.205	0.233	0.260	0.259	0.191	0.207	0.201	0.187	0.203	0.192	0.156
Liaoning	0.512	0.576	0.602	0.568	0.504	0.478	0.475	0.479	0.515	0.480	0.321
Nei Mongol	0.154	0.170	0.200	0.174	0.175	0.180	0.191	0.178	0.177	0.186	0.152
Ningxia	0.234	0.208	0.273	0.225	0.258	0.241	0.350	0.349	0.306	0.242	0.209
Qinghai	0.079	0.085	0.077	0.080	0.079	0.088	0.083	0.091	0.096	0.082	0.086
Shaanxi	0.357	0.301	0.401	0.324	0.261	0.269	0.338	0.304	0.315	0.246	0.224
Shandong	1.197	1.309	1.531	1.315	1.113	1.188	1.323	1.232	1.191	0.870	0.592
Shanghai	0.874	0.744	0.883	0.828	0.588	0.656	0.544	0.460	0.507	0.325	0.202
Shanxi	0.748	0.806	0.928	0.779	0.593	0.612	0.789	0.703	0.661	0.614	0.493
Sichuan	0.429	0.429	0.513	0.376	0.415	0.427	0.394	0.293	0.350	0.198	0.123
Taiwan	0.089	0.071	0.081	0.085	0.074	0.090	0.074	0.055	0.086	0.052	0.051
Tianjin	1.197	1.344	1.577	1.132	1.217	1.289	1.176	1.140	1.150	1.005	0.708
Xinjiang U.	0.073	0.074	0.087	0.093	0.088	0.094	0.090	0.090	0.111	0.101	0.084
Xizang/Tibet	0.080	0.097	0.086	0.091	0.094	0.111	0.096	0.097	0.083	0.087	0.087
Yunnan	0.140	0.159	0.182	0.147	0.144	0.153	0.149	0.131	0.127	0.100	0.085
Zhejiang	0.383	0.337	0.452	0.395	0.297	0.316	0.403	0.258	0.321	0.212	0.158
P.R. China	0.397	0.392	0.444	0.373	0.330	0.342	0.358	0.335	0.332	0.280	0.225

Table A2. Annual NO_x emissions (Gg N year^{-1}) per province in the domain of DECSO (in parentheses the fraction of provincial area considered) derived from OMI observations.

Province	2007	2008	2009	2010	2011	2012	2013	2014	2015
Anhui	167	169	187	224	242	292	288	282	215
Beijing	91	62	90	107	88	80	89	74	64
Chongqing	54	57	70	75	87	95	96	100	70
Fujian	96	114	100	114	161	162	153	167	137
Gansu (61 %)	31	38	37	42	61	73	60	78	52
Guangdong	383	383	331	341	371	413	360	374	331
Guangxi	118	148	118	145	152	224	224	200	157
Guizhou	107	130	142	154	131	194	191	180	122
Hainan	8	13	11	17	23	22	25	37	30
Hebei	427	423	403	515	563	543	544	511	436
Heilongjiang (74 %)	33	36	30	25	43	54	40	49	31
Henan	334	347	370	445	470	481	491	433	315
Hubei	135	140	144	186	248	263	233	270	199
Hunan	109	112	124	162	163	216	184	218	187
Jiangsu	374	344	344	421	470	433	428	445	365
Jiangxi	51	58	65	73	85	105	111	150	112
Jilin	30	22	18	20	45	50	43	48	43
Liaoning	122	128	124	169	205	225	178	199	173
Nei Mongol (83 %)	98	116	117	156	215	215	169	142	111
Ningxia	30	34	32	41	75	72	66	61	36
Shaanxi	118	118	113	181	216	222	196	208	158
Shandong	464	510	493	629	689	677	731	712	580
Shanghai	96	103	101	95	109	75	83	93	84
Shanxi	292	284	253	328	397	395	373	313	260
Sichuan (51 %)	155	158	179	204	232	254	271	280	205
Taiwan	100	106	98	106	113	118	106	114	111
Tianjin	77	86	99	136	152	114	102	97	88
Yunnan (36 %)	83	109	105	97	118	159	144	176	126
Zhejiang	243	253	247	270	327	281	294	292	240
East China	4332	4502	4454	5382	6150	6402	6179	6201	4941

Competing interests. The authors declare that they have no conflict of interest.

Acknowledgements. This research was funded by the MarcoPolo project of the European Union Seventh Framework Programme (FP7/2007-2013) under grant agreement no. 606953 and by the GlobEmission project (contract no. 4000104001/11/I-NB) of the Data User Element programme of the European Space Agency.

Edited by: G. Frost
Reviewed by: two anonymous referees

References

Boersma, K. F., Eskes, H. J., Dirksen, R. J., van der A, R. J., Veefkind, J. P., Stammes, P., Huijnen, V., Kleipool, Q. L., Sneep, M., Claas, J., Leitão, J., Richter, A., Zhou, Y., and Brunner, D.: An improved tropospheric NO_2 column retrieval algorithm for the Ozone Monitoring Instrument, Atmos. Meas. Tech., 4, 1905–1928, doi:10.5194/amt-4-1905-2011, 2011.

Boersma, K. F., Vinken, G. C. M., and Tournadre, J.: Ships going slow in reducing their NO_x emissions: changes in 2005–2012 ship exhaust inferred from satellite measurements over Europe, Environ. Res. Lett., 10, 074007, doi:10.1088/1748-9326/10/7/074007, 2015.

Brenot, H., Theys, N., Clarisse, L., van Geffen, J., van Gent, J., Van Roozendael, M., van der A, R., Hurtmans, D., Coheur, P.-F., Clerbaux, C., Valks, P., Hedelt, P., Prata, F., Rasson, O., Sievers, K., and Zehner, C.: Support to Aviation Control Service (SACS): an online service for near-real-time satellite monitoring of volcanic plumes, Nat. Hazards Earth Syst. Sci., 14, 1099–1123, doi:10.5194/nhess-14-1099-2014, 2014.

CAAC: Clean Air Alliance of China, State Council air pollution prevention and control action plan, issue II, October 2013, available at: http://en.cleanairchina.org/product/6346.html (English translation), (last access: 8 October 2015), 2013.

Chen, W. and Xu, R.: Clean coal technology development in China, Energ. Policy, 38, 2123–2130, doi:10.1016/j.enpol.2009.06.003, 2010.

ChinaFAQs Project: China Adopts World-Class Pollutant Emissions Standards for Coal Power Plants, available at: http://www.chinafaqs.org/library/chinafaqs-china-adopts (last access: 8 October 2015), 2012.

de Foy, B., Lu, Z., and Streets, D. G.: Satellite NO_2 retrievals suggest China has exceeded its NO_x reduction goals from the twelfth Five-Year Plan, Scientific Reports, 6, 35912, doi:10.1038/srep35912, 2016.

De Ruyter de Wildt, M., Eskes, H., and Boersma, K. F.: The global economic cycle and satellite-derived NO_2 trends over shipping lanes, Geophys. Res. Lett., 39, L01802, doi:10.1029/2011GL049541, 2012.

Ding, J., van der A, R. J., Mijling, B., Levelt, P. F., and Hao, N.: NO_x emission estimates during the 2014 Youth Olympic Games in Nanjing, Atmos. Chem. Phys., 15, 9399–9412, doi:10.5194/acp-15-9399-2015, 2015.

Ding, J., van der A, R. J., Mijling, B., and Levelt, P. F.: Space-based NO_x emission estimates over remote regions improved in DECSO, Atmos. Meas. Tech. Discuss., doi:10.5194/amt-2016-295, in review, 2016a.

Ding, J., van der A, R. J., and Mijling, B.: DECSO NO_x emissions (version 4), available at: http://www.globemission.eu/region_asia/datapage.php, 2016b.

Duncan, B. N., Lamsal, L. N., Thompson, A. M., Yoshida, Y., Lu, Z., Streets, D. G., Hurwitz, M. M., and Pickering, K. E.: A space-based, high-resolution view of notable changes in urban NO_x pollution around the world (2005–2014), J. Geophys. Res. 121, 976–96, 2016.

Eisinger, M. and Burrows, J. P.: Tropospheric sulfur dioxide observed by the ERS-2 GOME instrument, Geophys. Res. Lett., 25, 4177–4180, 1998.

Faber, J., Nelissen, D., Hon, G., Wang, H., and Tsimplis, M.: Regulated slow steaming in maritime transport – an assessment of options, costs and benefits CE Delft (the Netherlands: Delft), available at: www.cedelft.eu/publicatie/regulated_slow_steaming_in_maritime_transport/1224 (last access: 9 December 2016), 117 pp., 2012.

Fioletov, V. E., McLinden, C. A., Krotkov, N., and Li, C.: Lifetimes and emissions of SO_2 from point sources estimated from OMI, Geophys. Res. Lett., 42, 1969–1976, doi:10.1002/2015GL063148, 2015.

Fioletov, V. E., McLinden, C. A., Krotkov, N., Li, C., Joiner, J., Theys, N., Carn, S., and Moran, M. D.: A global catalogue of large SO_2 sources and emissions derived from the Ozone Monitoring Instrument, Atmos. Chem. Phys., 16, 11497–11519, doi:10.5194/acp-16-11497-2016, 2016.

Gu, D., Wang, Y., Smeltzer, C., and Liu, Z.: Reduction in NO_x emission trends over China: regional and seasonal variations, Environ. Sci. Technol., 47, 12912–12919, 2013.

Guan, D., Liu, Z., Geng, Y., Lindner, S., and Hubacek, K.: The gigatonne gap in China's carbon dioxide inventories, Nature Climate Change, 2, 672–675, doi:10.1038/nclimate1560, 2012.

Hong, C., Zhang, Q., He, K., Guan, D., Li, M., Liu, F., and Zheng, B.: Variations of China's emission estimates response to uncertainties in energy statistics, Atmos. Chem. Phys. Discuss., doi:10.5194/acp-2016-459, in review, 2016.

He, K.: Multi-resolution Emission Inventory for China (MEIC): model framework and 1990–2010 anthropogenic emissions, in International Global Atmospheric Chemistry Conference, 17–21 September, Beijing, China, available at: http://adsabs.harvard.edu/abs/2012AGUFM.A32B..05H (last access: 4 February 2015), 2012.

He, H., Li, C., Loughner, C. P., Li, Z., Krotkov, N. A., Yang, K., Wang, L., Zheng, Y., Bao, X., Zhao, G., and Dickerson, R. R.: SO_2 over central China: Measurements, numerical simulations and the tropospheric sulfur budget, J. Geophys. Res., 117, D00K37, doi:10.1029/2011JD016473, 2012.

ICAC: Institute of Clean Air Companies, Selective Catalytic Reduction (SCR) control of NO_x emissions from fossil fuel-fired electric power plants, available at: https://c.ymcdn.com/sites/icac.site-ym.com/resource/resmgr/Standards_WhitePapers/SCR_WhitePaper_final_2009.pdf (last access: 22 November 2016), 2009.

Irie, H., Muto, T., Itahashi, S., Kurokawa, J., and Uno, I.: Turnaround of tropospheric nitrogen dioxide pollution trends in China, Japan, and South Korea, SOLA, 12, 170–174, doi:10.2151/sola.2016-035, 2016.

Klimont, Z., Smith, S. J., and Cofala, J.: The last decade of global anthropogenic sulfur dioxide: 2000–2011 emissions, Environ. Res. Lett., 8, 014003, doi:10.1088/1748-9326/8/1/014003, 2013.

KNMI: Background information about the Row Anomaly in OMI, available at: http://www.knmi.nl/omi/research/product/rowanomaly-background.php (last access: 8 October 2015), 2012.

Koukouli, M. E., Balis, D. S., van der A, R. J., Theys, N., Hedelt, P., Richter, A., Krotkov, N., Li, C., and Taylor, M.: Anthropogenic sulphur dioxide load over China as observed from different satellite sensors, Atmos. Environ., 145, 45–59, doi:10.1016/j.atmosenv.2016.09.007, 2016.

Krotkov, N. A., Carn, S. A., Krueger, A. J., Bhartia, P. K., and Yang, K.: Band residual difference algorithm for retrieval of SO_2 from the aura ozone monitoring instrument (OMI), IEEE T. Geosci. Remote, 44, 1259–1266, doi:10.1109/TGRS.2005.861932, 2006.

Krotkov, N. A., McLinden, C. A., Li, C., Lamsal, L. N., Celarier, E. A., Marchenko, S. V., Swartz, W. H., Bucsela, E. J., Joiner, J., Duncan, B. N., Boersma, K. F., Veefkind, J. P., Levelt, P. F., Fioletov, V. E., Dickerson, R. R., He, H., Lu, Z., and Streets, D. G.: Aura OMI observations of regional SO_2 and NO_2 pollution changes from 2005 to 2015, Atmos. Chem. Phys., 16, 4605–4629, doi:10.5194/acp-16-4605-2016, 2016.

Kurokawa, J. I., Yumimoto, K., Uno, I., andOhara, T.: Adjoint inverse modeling of NO_x emissions over eastern China using satellite observations of NO_2 vertical column densities, Atmos. Environ., 43, 1878–1887, 2009.

Kurokawa, J., Ohara, T., Morikawa, T., Hanayama, S., Janssens-Maenhout, G., Fukui, T., Kawashima, K., and Akimoto, H.: Emissions of air pollutants and greenhouse gases over Asian regions during 2000–2008: Regional Emission inventory in ASia (REAS) version 2, Atmos. Chem. Phys., 13, 11019–11058, doi:10.5194/acp-13-11019-2013, 2013.

Lee, C., Richter, A., Weber, M., and Burrows, J. P.: SO_2 Retrieval from SCIAMACHY using the Weighting Function DOAS (WF-DOAS) technique: comparison with Standard DOAS retrieval, Atmos. Chem. Phys., 8, 6137–6145, doi:10.5194/acp-8-6137-2008, 2008.

Lee, C., Martin, R. V., van Donkelaar, A., Lee, H., Dickerson, R. R., Hains, J. C., Krotkov, N., Richter, A., Vinnikov, K., and Schwab, J. J.: SO_2 emissions and lifetimes: Estimates from inverse modeling using in situ and global, space-based (SCIAMACHY and OMI) observations, J. Geophys. Res., 116, D06304, doi:10.1029/2010JD014758, 2011.

Levelt, P. F., van den Oord, G. H. J., Dobber, M. R., Mälkki, A., Visser, H., de Vries, J., Stammes, P., Lundell, J., and Saari, H.: The ozone monitoring instrument, IEEE T. Geosci. Remote, 44, 1093–1101, doi:10.1109/TGRS.2006.872333, 2006.

Li, C., Zhang, Q., Krotkov, N. A., Streets, D. G., He, K., Tsay, S.-C., and Gleason, J. F.: Recent large reduction in sulfur dioxide emissions from Chinese power plants observed by the Ozone Monitoring Instrument, Geophys. Res. Lett., 37, 1–6, doi:10.1029/2010GL042594, 2010.

Lin, J.-T. and McElroy, M. B.: Detection from space of a reduction in anthropogenic emissions of nitrogen oxides during the Chinese economic downturn, Atmos. Chem. Phys., 11, 8171–8188, doi:10.5194/acp-11-8171-2011, 2011.

Liu, F., Zhang, Q., Tong, D., Zheng, B., Li, M., Huo, H., and He, K. B.: High-resolution inventory of technologies, activities, and emissions of coal-fired power plants in China from 1990 to 2010, Atmos. Chem. Phys., 15, 13299–13317, doi:10.5194/acp-15-13299-2015, 2015.

Liu, F., Beirle, S., Zhang, Q., Dörner, S., He, K., and Wagner, T.: NO_x lifetimes and emissions of cities and power plants in polluted background estimated by satellite observations, Atmos. Chem. Phys., 16, 5283–5298, doi:10.5194/acp-16-5283-2016, 2016a.

Liu, F., Zhang, Q., van der A, R. J., Zheng, B., Tong, D., Yan, L., and He, K. B.: Recent reduction in NO_x emissions over China from satellite observations and emission inventories, Env. Res. Lett., submitted, 2016b.

Lu, Z., Streets, D. G., Zhang, Q., Wang, S., Carmichael, G. R., Cheng, Y. F., Wei, C., Chin, M., Diehl, T., and Tan, Q.: Sulfur dioxide emissions in China and sulfur trends in East Asia since 2000, Atmos. Chem. Phys., 10, 6311–6331, doi:10.5194/acp-10-6311-2010, 2010.

McLinden, C. A., Fioletov, V., Shephard, M. W., Krotkov, N., Li, C., Martin, R. V., Moran, M. D., and Joiner, J.: Space-based detection of missing sulfur dioxide sources of global air pollution, Nat. Geosci, 9, 496–500, doi:10.1038/ngeo2724, 2016.

Menut, L., Bessagnet, B., Khvorostyanov, D., Beekmann, M., Blond, N., Colette, A., Coll, I., Curci, G., Foret, G., Hodzic, A., Mailler, S., Meleux, F., Monge, J.-L., Pison, I., Siour, G., Turquety, S., Valari, M., Vautard, R., and Vivanco, M. G.: CHIMERE 2013: a model for regional atmospheric composition modelling, Geosci. Model Dev., 6, 981–1028, doi:10.5194/gmd-6-981-2013, 2013.

MEP: Ministry of Environmental Protection, available at: http://english.mep.gov.cn/Plans_Reports/, last access: 8 October 2015.

Mijling, B. and van der A, R. J.: Using daily satellite observations to estimate emissions of short-lived air pollutants on a mesoscopic scale, J. Geophys. Res., 117, D17302, doi:10.1029/2012JD017817, 2012.

Mijling, B., van der A, R. J., Boersma, K. F., Van Roozendael, M., De Smedt, I., and Kelder, H. M.: Reduction of NO_2 detected from space during the 2008 Beijing Olympic Games, Geophys. Res. Lett., 36, L13801, doi:10.1029/2009GL038943, 2009.

Mijling, B., van der A, R. J., and Zhang, Q.: Regional nitrogen oxides emission trends in East Asia observed from space, Atmos. Chem. Phys., 13, 12003–12012, doi:10.5194/acp-13-12003-2013, 2013.

Munro, R., Lang, R., Klaes, D., Poli, G., Retscher, C., Lindstrot, R., Huckle, R., Lacan, A., Grzegorski, M., Holdak, A., Kokhanovsky, A., Livschitz, J., and Eisinger, M.: The GOME-2 instrument on the Metop series of satellites: instrument design, calibration, and level 1 data processing – an overview, Atmos. Meas. Tech., 9, 1279–1301, doi:10.5194/amt-9-1279-2016, 2016.

NBSC: National Bureau of Statistics China, available at: http://data.stats.gov.cn, last access: 29 December 2015.

NDRC: National Development and Reform Commission, available at: http://www.ndrc.gov.cn/zcfb/zcfbtz/201308/t20130827_555124.html (last access: 1 November 2015), reported on 16 August 2013.

Richter, A., Burrows, J. P., Nüß, H., Granier, C., and Niemeier, U.: Increase in tropospheric nitrogen dioxide over China observed from space, Nature, 437, 129–132, doi:10.1038/nature04092, 2005.

Schneider, P., Lahoz, W. A., and van der A, R.: Recent satellite-based trends of tropospheric nitrogen dioxide over large urban agglomerations worldwide, Atmos. Chem. Phys., 15, 1205–1220, doi:10.5194/acp-15-1205-2015, 2015.

State Council: State Council announcement on 15 May 2014 of environmental regulations), available at: http://www.gov.cn/zhengce/content/2014-05/26/content_8824.htm (last access: 1 November 2015), 2014.

Stavrakou, T., Müller, J. F., Boersma, K. F., De Smedt, I., and van der A, R. J.: Assessing the distribution and growth rates of NO_x emission sources by inverting a 10-year record of NO_2 satellite columns, Geophys. Res. Lett., 35, L10801, doi:10.1029/2008GL033521, 2008.

Sun, L. and Zhou, N. (Eds.): Guizhou power supply tight, Xinhua News Agency, available at: http://news.xinhuanet.com/fortune/2011-10/22/c_111115420.htm (last access: 9 December 2016), 22 October 2011.

Theys, N., De Smedt, I., van Gent, J., Danckaert, T., Wang, T., Hendrick, F., Stavrakou, T., Bauduin, S., Clarisse, L., Li, C., Krotkov, N., Yu, H., Brenot, H., and Van Roozendael, M.: Sulfur dioxide vertical column DOAS retrievals from the Ozone Monitoring Instrument: global observations and comparison to ground-based and satellite data, J. Geophys. Res.-Atmos., 120, 2470–2491, doi:10.1002/2014JD022657, 2015.

van der A, R. J., Peters, D. H. M. U., Eskes, H., Boersma, K. F., Van Roozendael, M., De Smedt, I., and Kelder, H. M.: Detection of the trend and seasonal variation in tropospheric NO_2 over China, J. Geophys. Res., 111, D12317, doi:10.1029/2005JD006594, 2006.

Valks, P. J. M.: GOME-2/Metop-A SO2 data (version GDP 4.7), available at: http://atmos.caf.dlr.de/gome2/, 2016.

Wu, Y., Zhang, S., Hao, J., Liu, H., Wu, X., Hu, J., Walsh, M. P., Wallington, T. J., and Zhang, K. M. S.: Stevanovic, On-road vehicle emissions and their control in China: A review and outlook, Sci. Total Environ., 574, 332–349, doi:10.1016/j.scitotenv.2016.09.040, 2017.

Xu, Y.: Improvements in the Operation of SO_2 Scrubbers in China's Coal Power Plants, Environ. Sci. Technol., 45, 380–385, doi:10.1021/es1025678, 2011.

Yang, K., Dickerson, R. R., Carn, S. A., Ge, C., and Wang, J.: First observations of SO_2 from the satellite Suomi NPP OMPS: Widespread air pollution events over China, Geophys. Res. Lett., 40, 4957–4962, doi:10.1002/grl.50952, 2013.

Zhang, Q., Geng, G., Wang, S., Richter, A., and He, K.: Satellite remote sensing of changes in NO $\times$ emissions over China during 1996–2010, Chinese Sci. Bull., 57, 2857–2864, 2012.

Zhang, R.: Heating causes pollution spike in Northern China, CCTV.com, available at: http://english.cntv.cn/program/china24/20131108/101015.shtml (last access: 9 December 2016), 11 August 2013.

Zhao, B., Wang, S. X., Liu, H., Xu, J. Y., Fu, K., Klimont, Z., Hao, J. M., He, K. B., Cofala, J., and Amann, M.: NOx emissions in China: historical trends and future perspectives, Atmos. Chem. Phys., 13, 9869–9897, doi:10.5194/acp-13-9869-2013, 2013.

Zhu, N.: China to shut coal mines in safety overhaul, Xinhua News Agency, available at: http://news.xinhuanet.com/english/china/2013-10/12/c_132793667.htm (last access: 9 December 2016), 12 October 2013.